CHAPTER III
A PHYSIOLOGICALLY BASED MODEL FOR ETHANOL AND ACETALDEHYDE METABOLISM IN HUMAN BEINGS

3.1 Abstract

Pharmacokinetic models for ethanol metabolism have contributed to our understanding of ethanol clearance in human beings. However, these models fail to account for ethanol's toxic metabolite acetaldehyde. Acetaldehyde accumulation causes symptoms such as cardiac arrhythmia, nausea, anxiety and facial flushing. Nevertheless, it is difficult to determine the levels of acetaldehyde in the blood or other tissues due to artefactual formation and other technical issues. Therefore, we have constructed a promising physiologically based pharmacokinetic (PBPK) model, which is an excellent match for existing ethanol and acetaldehyde concentration-time data. Specifically, the model consists of five compartments that exchange material: stomach, gastrointestinal tract, liver, central fluid, and muscle. All compartments are modeled as stirred reactors except the liver, which is modeled as a tubular flow reactor. We derived average enzymatic rate laws for alcohol (ADH) and acetaldehyde dehydrogenases (ALDH), determined kinetic parameters from the literature and found best-fit parameters by minimizing the squared error between our profiles and the experimental data. The model's transient output correlates strongly with the experimentally observed results for normal individuals and for those with reduced acetaldehyde dehydrogenase activity caused by a genetic deficiency of the primary acetaldehyde metabolizing enzyme *ALDH2*. Furthermore, the model shows that the reverse reaction of acetaldehyde back into ethanol is essential and keeps acetaldehyde levels approximately 10 fold lower than if the reaction were irreversible.

Keywords: Alcohol metabolism; Acetaldehyde dehydrogenase (ALDH); ALDH deficiency; Physiologically based pharmacokinetic (PBPK) model; Alcohol dehydrogenase (ADH); Michaelis-Menten (M-M) kinetics

3.2 Introduction

Pharmacokinetic models for in vivo ethanol elimination have evolved significantly over the past 70 years, from the inception of a pseudo-zero order elimination process Widmark (1932), to the current physiologically based models such as those developed by (Derr, 1993; Levitt, 2002; Norberg, 2001). While the models continually improve in their ability to predict time trajectories for ethanol concentration, they fail to account for the production and interaction of ethanol's major metabolite, acetaldehyde. Acetaldehyde is highly toxic with an LD_{50} concentration ~10 times lower than ethanol in rats (Brien & Loomis, 1983). Acetaldehyde exposure leads to a number of well-known symptoms such as cardiac arrhythmias, nausea, anxiety, and facial flushing (Condouris & Havelin, 1987; Peng et al., 1999; Yamamoto et al., 2000). This paper presents a physiologically based model with reversible enzyme kinetics that accurately predicts simultaneously the concentrations of both ethanol and acetaldehyde in the blood as a function of time.

3.3 Methods

3.3.1 Rate law derivation

The rate law for ethanol metabolism is based on the alcohol dehydrogenase (ADH) reaction pathway because it is the largest contributor to ethanol oxidation. The first assumption is that the concentration of NAD^+ reaches its rate limiting state shortly after ingestion and remains constant. Ethanol elimination is approximately zeroth order, suggesting that the reaction is limited by the amount of enzyme and/or co-substrate. The enzymatic reaction, accounting for the NAD^+ co-substrate is:

$$r_{Al} = \frac{V_m^*(S_1)(S_2)}{K_{12} + K_1(S_1) + K_2(S_2) + (S_1)(S_2)} \quad \text{where } S_1 \equiv C_{Alcohol}, \text{ and } S_2 \equiv C_{NAD^+}.$$

Thus, since the elimination is approximately constant with rate V_{max}, two cases are possible: the rate occurs at $V_{max} = V_m$ when S_1 is >> K_2 and NAD^+ is either in excess such that $(K_{12}+K_1S_1)/S_2$ approaches zero or the rate occurs at $V_{max} = f(S_2)$ and S_2

reaches a limiting concentration dependent upon the rate that it is replenished to the system. Here, the experimentally observed K_M and V_{max} depend on the steady-state concentration of NAD^+.

$$r_{Al} = \frac{\frac{V_m(S_2)}{K_1+(S_2)} * (S_1)}{\frac{K_{12}+K_2(S_2)}{K_1+(S_2)} + (S_1)} \quad \text{where } K_M \equiv \frac{K_{12}+K_2(S_2)}{K_1+(S_2)}. \text{ and } V_{max'} \equiv \frac{V_{max}(S_2)}{K_1+(S_2)}$$

It is most likely that the concentration of NAD^+ is limiting but the exact levels are not necessary for this study. Instead, it is worth noting that V_{max} and K_m depend upon the steady-state concentrations of NAD^+. The second assumption is that the net rate of formation of the substrate-enzyme complex is zero. Consequently, we can apply the pseudo steady-state hypothesis (PSSH) to the enzyme-ethanol and enzyme-acetaldehyde complexes (Fogler, 1999).

The derivation of the rate law for acetaldehyde oxidation is similar to the derivation for ethanol oxidation with one major exception: acetaldehyde oxidation to acetate is not reversible. The rate law is based on the aldehyde dehydrogenase (*ALDH2*) enzymatic pathway because it is the largest contributor to acetaldehyde oxidation. In normal human beings, *ALDH2* activity alone accounts for over 99% of acetaldehyde oxidation (Riveros-Rosas et al., 1997). *ALDH2* uses the same co-substrate, NAD^+, as ADH and therefore it is assumed to reach its rate limiting state rapidly and to remain constant at that level. The derivation of the acetaldehyde oxidation rate-law is also based upon application of the PSSH to the enzyme-substrate complexes. The balance equations and rate law derivation are shown in Fig. 3.1A (Fogler, 1999).

<Fig. 3.1>

C_{Al} is the ethanol concentration, and C_{Ac} is the acetaldehyde concentration. V_{maxADH} is the maximum enzymatic oxidation rate of ethanol, V_{revADH} is the maximum rate of the reverse reaction of acetaldehyde to ethanol, K_{mADH} and K_{revADH} are reaction constants for the rate law. The rate-law for acetaldehyde oxidation is dependent only on the concentration of acetaldehyde and follows classical Michaelis-Menten kinetics.

3.3.2 Physiologically Based Model

We consider our system to be lumped into five organ compartments that exchange material. The five compartments are the stomach, gastrointestinal tract, liver, muscle and central fluid. The stomach compartment in this model contains zero tissue water volume and only the volume of the liquid contents (alcoholic beverage), which is absorbed into the gastrointestinal (GI) compartment. The GI compartment accounts for the tissue water volume of the intestines and the stomach where ethanol is first absorbed. We chose to separate the GI compartment from the central compartment based on the physiological connectivity. This separation also establishes a base case model that can easily be extended to studies on the GI tract's role in first-pass metabolism. A perfusion-limited model was selected because both ethanol and acetaldehyde are small molecules with rapid diffusion and their distribution is limited by the rate they are transported to the tissues and not the rate at which they are absorbed.

Physiologically based models have available to them the human approximations for tissue water volume, perfusion rates, and tissue water distribution (well-mixed vs. concentration gradient). Such data are given in Table 3.1 for a "standard" 69.4 kg male whose total body water content (TBW) is 40.8 liters (Rowland & Tozer, 1995).

<Table 3.1.>

To accurately describe ethanol and acetaldehyde metabolism in vivo, we divided the total tissue water volume (TWV) of an average 69.4 kg male human being into three well-mixed compartments and one tubular flow compartment. Organ volumes were lumped into compartments based on three criteria: 1) perfusion rate of fluid through each organ, 2) the physical connectivity between organs, and 3) ethanol and acetaldehyde metabolic activity. The perfusion rate is defined as the flow rate to and from the organ per unit volume of tissue and the inverse of the perfusion rate is the residence time. Ethanol and acetaldehyde metabolism occurs

within the liver, which was considered as a tubular flow reactor based on early kinetic results obtained by (Keiding & Priisholm, 1984). The stomach and intestine water volumes were grouped into the gastrointestinal (GI) compartment because they are connected directly to the liver via the hepatic portal vein and because they are the site of ethanol absorption from an external source. Finally, organs with a perfusion rate > 0.08 ml/min/mlH_2O were placed within the central compartment while organs with perfusion rates < 0.08 were placed within the muscle compartment.

Mass balance equations with the appropriate reaction rate laws were constructed based on the flow of blood between compartments and are shown in Fig. 3.1B. The compartment labeled "Stomach" contains the ethanol that is external to the body and represents the volume of the liquid contents (alcoholic beverage) which are absorbed into the GI compartment. Fig. 3.2A shows the compartment/flow diagram for the model. The rate of stomach emptying determined using radiopharmaceuticals by Levitt & Levitt (1994), can be approximated by a 1st order linear ordinary differential equation where the rate of removal is proportional to the volume of stomach contents (Levitt & Levitt, 1994). However, the stomach-emptying rate constant depends upon the osmotic pressure of the stomach contents and ethanol increases the osmotic pressure. Wilkinson et al. (1977), results of studies shown that the rate constant is a non-linear function of the initial dose of ethanol ingested. The equation previously proposed and used for this work is $k_S = k_{Smax}/(1+a(D)^2)$ where k_S is the stomach emptying rate constant, k_{Smax} is the maximum stomach-emptying rate constant, a is an empirical parameter, and D is the initial dose of ethanol in the stomach (mmol) (Wilkinson et al., 1977).

It is very difficult to determine the concentration of free acetaldehyde in the blood based on either breath or blood analysis methods. Artefactual formation of acetaldehyde inhibits accurate blood analysis and production of acetaldehyde by micro-organisms in the throat inhibits acetaldehyde determination from breath assays (Jones, 1995). Much of the acetaldehyde present in the blood is bound to plasma proteins and hemoglobin, and only the unbound acetaldehyde crosses the alveolar-capillary membranes of the lungs and great care must be taken to ensure one is actually measuring free acetaldehyde. Breath tests give an approximation of free acetaldehyde in the blood; however random errors in the assay used detract from the

ability to accurately calculate blood acetaldehyde concentrations from breath levels. Noting these problems, breath acetaldehyde data were used in our initial analysis. To verify and test the model further, we compared our theoretical results with data obtained more recently by blood analysis in Asian men where recent protocols were used to reduce artefactual formation of acetaldehyde (Peng et al., 1999).

3.4 Results and discussion

3.4.1 Parameter values

The commercial technical computing package Matlab® was used for model development and parameter estimation. The differential balances on each compartment along with the appropriate enzymatic rate laws were solved numerically with Matlab®'s stiff ordinary differential equation solvers due to the large difference in the ethanol and acetaldehyde concentrations (Shampine & Reichelt, 1997). Two realizations were carried out: (1) the model parameter values for the balance equations and rate laws were taken directly from the average literature values, and (2) the model parameters were fit to the experimental concentration-time trajectories available in the literature. All parameter estimations were carried out by utilizing Matlab®'s built-in routines from its optimization toolbox. A least-square criterion between average experimental values and model output was used. As one can observe in Fig. 3.2B, 3.2C, and 3.2D, there is little variation between these two realizations. The model parameters are shown in Table 3.2. Due to the lack of a firmly established value, the Michaelis-Menten parameter V_{maxAc} was taken to be 2.7 mmol/(min*kg liver) which is within the range of the suggested values (Deetz et al., 1984).

<Table 3.2.>

In addition to the parameters in Table 3.2, k_{Smax} and a were fit to the model. Values of 0.05 min^{-1} and 1.22 mol^{-2} were obtained for k_{Smax} and a respectively.

Using these values for k_{Smax} and a we obtained the following overall stomach emptying rate constants compared with those from (Wilkinson et al., 1977).

<Table 3.3.>

The absorption rate is much less dependent on the concentration of ethanol in the current model. In fact, for the 0.6 g ethanol/kg dose the current work results of our studies indicate that 92% of the ethanol is absorbed within 100 minutes whereas in the one-compartment model only 39% of the ethanol is absorbed. Even with very slow absorption rates, greater than 80% absorption is expected to occur within 100 minutes (Levitt & Levitt 1994; Levitt et al., 1997).

3.4.2 Ethanol concentrations

Fig. 3.2B shows a comparison of the ethanol concentration-time trajectories for the central compartment with the data taken from (Wilkinson et al., 1977). The four curves correspond to four different doses of ethanol of 0.15, 0.3, 0.45, and 0.6 g/kg body weight being administered. One notes that in all cases, there is excellent agreement between theory and experiment and also that the parameters taken from the literature give virtually the same result as those found by the least squares fit.

<Fig. 3.2>

The correlation between the model predictions and experimental observations is excellent for ethanol with an r^2 value of 0.98. One readily observes the model accurately predicts the ethanol concentration-time trajectory using physiologically relevant parameters.

3.4.3 Alcohol dehydrogenase reverse reaction

The reverse reaction for acetaldehyde to ethanol in the blood is favored 5-50 times over acetaldehyde based on in vitro calculations, supporting the notion of a

significant reverse reaction effect (Deetz et al., 1984). In order to determine acetaldehyde's influence on the removal of ethanol, we considered the data of Jones et al. (1988), who administered calcium carbimide in volunteers to slow the rate of acetaldehyde metabolism before giving them a dose of ethanol equivalent to 0.25 g ethanol (96%)/kg body weight (Jones et al., 1988). In order to calculate the value for the reverse reaction enzymatic activity parameter, V_{rev}, it was assumed that the concentration of acetaldehyde in the liver is equal to the concentration of acetaldehyde in the central compartment at time t. This approximation was made due to the lack of available data, and it introduces a minor amount of systematic error to our least-squares fit estimate for V_{rev}. Fig. 3.2C shows a comparison of the suppressed metabolism and normal metabolism along with the model prediction for each case. Theory and experiment are in good agreement and the correlation between the model-predicted and experimentally-observed results for the regular ethanol and calcium carbimide inhibited *ALDH2* cases have r^2 values of 0.99 and 0.89 respectively.

3.4.4 Acetaldehyde concentration

As discussed earlier, one of the salient features of the current model is that it can simultaneously predict the concentration-time trajectories for ethanol and acetaldehyde when they are measured simultaneously. Fig. 3.2C shows the ethanol comparison and Fig. 3.2D shows the acetaldehyde comparison. There was no adjustment of parameter values for the different concentration trajectories. The results for blood acetaldehyde concentration–time trajectories predicted by the model are compared with experimental results obtained by Jones et al. (1988), after 0.25 g/kg 96% ethanol dose. Again, the agreement between the experiment measurements and the model is excellent. A correlation between the model-predicted and observed results for acetaldehyde is good with an r^2 value of 0.88.

3.4.5 Acetaldehyde dehydrogenase deficiency

Another primary feature of the current model is its application to aldehyde dehydrogenase deficient individuals in order to predict the acetaldehyde concentration-time trajectory. Acetaldehyde dehydrogenase activity in the liver was calculated using data from Enomoto et al. (1991), based on the percent change from the normal activity. Enomoto et al. (1991), showed that the total ALDH specific activity for acetaldehyde metabolism (V_{maxAc}) in heterozygous *ALDH2*1/*2* individuals was only 70% of the total ALDH specific activity for acetaldehyde metabolism (V_{maxAc}) in homozygous *ALDH2*1/*1* individuals for low doses of ethanol. Additionally, the total ALDH specific activity for acetaldehyde metabolism (V_{maxAc}) in homozygous *ALDH2*2/*2* individuals was only 55% of the total ALDH specific activity for acetaldehyde metabolism (V_{maxAc}) in homozygous *ALDH2*1/*1* individuals. When we apply these percentages to our model V_{maxAc}, we get rates of 1.89 and 1.49 mmol*(min*kg liver)$^{-1}$ for *ALDH2*1/*2* and *ALDH2*2/*2* individuals respectively. The results for heterozygous *ALDH2*1/*2* individuals are in agreement with the results shown by (Wang et al., 1996). The Michaelis-Menten constant K_m was held constant and only V_{maxAc} was varied.

These parameters were used in the model and compared with the data from Peng et al. (1999), obtained by ethanol administration to *ALDH2*1/*1*, *ALDH2*1/*2*, and *ALDH2*2/*2* individuals (Peng et al., 1999; Wang et al., 1996). Additionally, the stomach-emptying rate constant was reduced to 50% of the normal absorption rate because the subjects ate breakfast approximately 2 hours before the study whereas other studies Wilkinson et al. (1977), and Jones et al. (1988), required an overnight fast. This is calculated based on the ethanol concentration time data taken by Lucey et al. (1999), after orally ingesting 0.3g/kg of ethanol in individuals after an overnight fast and eating a standard meal. The stomach emptying rate constant decreases by approximately 50% after orally ingesting 0.3g/kg ethanol after taking a standard meal. Plots of experimental data from Lucey et al. (1999), for fed and fasted state and model predicted curves are shown in Fig. 3.4D. Fig. 3.3 and Fig. 3.4A show the blood ethanol and blood acetaldehyde concentrations respectively.

<Fig. 3.3>

Fig. 3.4A shows acetaldehyde concentration-time trajectories for *ALDH2*1/*1* (bottom), *ALDH2*1/*2* (middle) and *ALDH2*2/*2* (top) individuals with data from Peng et al. (1999). As acetaldehyde concentration increases, the peak concentration becomes more distinct than seen in lower acetaldehyde concentrations where plateaus develop. Thus, as acetaldehyde concentration increases, the characteristic shape of the concentration-time trajectory for acetaldehyde more closely resembles the ethanol concentration-time trajectory and the reaction is limited by the rate of acetaldehyde removal. In normal *ALDH2*1/*1* individuals, the plateau shape is a result of the balance between the rate of acetaldehyde formation and removal from ethanol. Fig. 3.4B and Fig. 3.4C show the concentration-time trajectories for ethanol and acetaldehyde, respectively, with and without the reverse reaction accounted for in the rate law for ethanol. Neglecting the reverse reaction decreases the peak level and area under the curve (a measure of exposure) of ethanol while greatly increasing the exposure to acetaldehyde. Fig. 3.4D shows the concentration-time trajectories for ethanol after orally ingesting 0.3 g/kg of ethanol with an overnight fast and eating a standard meal.

<Fig. 3.4>

3.5 Conclusions

This work demonstrates, for the first time, simultaneous ethanol and acetaldehyde concentration-time profiles. The utility of the model lies in its ability to predict the correct acetaldehyde concentration profiles in different individuals under different experimental conditions when the initial dose and mass of the individual is known. The model least-squares parameters coincide strongly with those determined by in vitro experimentation. The high rate of reaction from acetaldehyde to ethanol via alcohol dehydrogenase plays a significant role in the kinetics of acetaldehyde and only a minor role in the kinetics of ethanol.

3.6 Appendix

3.6.1 Stomach compartment

Ethanol is primarily absorbed by the tissues of the first part of the small intestine (duodenum) and to a lesser extent the tissue lining the stomach (gastric mucosa). The rate of ethanol absorption by the duodenum is between 7.5 and 85 times greater than the rate ethanol enters the blood from the stomach (Wilkinson et al., 1977). Therefore, ethanol entering the duodenum is virtually instantaneously absorbed into the GI tissues and ethanol absorption by the duodenum can be approximated by the rate ethanol is emptied from the stomach into the duodenum. The first order relationship for the change in volume of fluid in the stomach, V_S, with respect to time is given by:

$$\left(\frac{dV_S}{dt}\right) = -k_S(V_S) \qquad \text{(A1)}$$

The stomach-emptying rate constant, k_S (min^{-1}), is dependent upon the initial dose D (mmol) of ethanol in the system.

3.6.2 Gastrointestinal compartment

The stomach contents are emptied into the gastrointestinal (GI) system, which has a tissue water volume of 2.4 l (Derr, 1993). The blood flow rate through the GI system is equal to the blood flow rate entering the liver via the hepatic portal vein. This flow rate is approximately 2/3 of the total blood flow rate to the liver, which is 1350 ml/min (Levitt & Levitt, 1994). A mass balance on the G.I compartment gives equations (A2) and (A3) for ethanol and acetaldehyde, respectively.

$$V_G \frac{dC_{GAl}}{dt} = \left(\frac{2}{3}v_L\right)(C_{CAl} - C_{GAl}) + k_S(V_S)(C_{SAl}) \qquad \text{(A2)}$$

$$V_G \frac{dC_{GAc}}{dt} = \left(\frac{2}{3}v_L\right)(C_{CAc} - C_{GAc}) \qquad \text{(A3)}$$

In equations (A2) and (A3), V_G is the GI system tissue water volume, v_L is the liver flow-rate, C_{GAl} and C_{CAl} are the GI and central compartment ethanol concentrations, respectively, and C_{GAc} and C_{CAc} are the GI and central compartment acetaldehyde concentrations, respectively.

3.6.3. Liver compartment

Ethanol in the blood flows through the hepatic portal vein to the liver after exiting the GI compartment. Additionally, the liver receives blood from the hepatic artery, which supplies the other 1/3 of the total hepatic blood flow rate. After entering the liver, ethanol is converted into acetaldehyde by the enzyme alcohol dehydrogenase and acetaldehyde into acetate by acetaldehyde dehydrogenase. Due to the complexity of the forward and reverse reactions in this system, an unsteady-state, physiologically based perfusion liver model is used. While an analytical solution for the case of irreversible Michaelis-Menten kinetics in a perfused liver is available (Bass et al., 1976), the log mean concentration assumption suggested in that work cannot be used for more complex rate laws with product concentration dependence such as the case presented here. When the tubular model (i.e. series of well mixed compartments) and well mixed model (i.e. one well mixed compartment) were compared the concentration time profiles for ethanol and acetaldehyde corresponded better to the experimental data, when using tubular model. Furthermore, results of earlier studies suggested that the rate of clearance and K_m values exhibited a dependence on flow-rate when data was fit to a well mixed compartment while the constants did not exhibit a dependence on flow rate when the perfusion limited liver model was used (Keiding & Priisholm, 1984). For these reasons, we decided to use the perfusion limited liver model and the general mass balance equation for the tubular flow compartment with reaction is:

$$\frac{\partial C}{\partial t} + v_L \frac{\partial C}{\partial V_L} = R(C) \quad \textit{with boundary condition } C(0,t) = \frac{1}{3} C_C(t) + \frac{2}{3} C_S(t) \qquad \text{(A4)}$$

C is the concentration of ethanol or acetaldehyde within the liver while C_C and C_S are the concentrations within the central and stomach compartments respectively. If a backward difference approximation to the spatial derivative is used, this partial differential equation is converted into a set of N ordinary differential equations. This is equivalent to a series of well mixed reactors where the output of one reactor becomes the input to the next reactor.

If liver volume is discretized into N differential volumes, equation A4 becomes equations A5 through A7 for ethanol and A8 through A10 for acetaldehyde.

$$Compartment\ L1: \quad \Delta V_L \frac{dC_{1Al}}{dt} = v_L\left(\frac{1}{3}C_{CAl} + \frac{2}{3}C_{GAl} - C_{1Al}\right) + r_{Al}(C_{1Al}, C_{1Ac})\Delta V_L \quad (A5)$$

$$Compartment\ L2: \quad \Delta V_L \frac{dC_{2Al}}{dt} = v_L(C_{1Al} - C_{2Al}) + r_{Al}(C_{2Al}, C_{2Ac})\Delta V_L \quad (A6)$$

$$\vdots$$

$$Compartment\ LN: \quad \Delta V_L \frac{dC_{NAl}}{dt} = v_L(C_{(N-1)Al} - C_{NAl}) + r_{Al}(C_{NAl}, C_{NAc})\Delta V_L \quad (A7)$$

$$Compartment\ L1: \quad \Delta V_L \frac{dC_{1Ac}}{dt} = v_L\left(\frac{1}{3}C_{CAc} + \frac{2}{3}C_{GAc} - C_{1Ac}\right) - r_{Al}(C_{1Al}, C_{1Ac})\Delta V_L + r_{Ac}(C_{1Ac})\Delta V_L \quad (A8)$$

$$Compartment\ L2: \quad \Delta V_L \frac{dC_{2Ac}}{dt} = v_L(C_{1Ac} - C_{2Ac}) - r_{Al}(C_{2Al}, C_{2Ac})\Delta V_L + r_{Ac}(C_{2Ac})\Delta V_L \quad (A9)$$

$$\vdots$$

$$Compartment\ LN: \quad \Delta V_L \frac{dC_{NAc}}{dt} = v_L(C_{(N-1)Ac} - C_{NAc}) - r_{Al}(C_{NAl}, C_{NAc})\Delta V_L + r_{Ac}(C_{NAc})\Delta V_L \quad (A10)$$

Ethanol and acetaldehyde exit the liver via the hepatic vein into the central compartment with concentrations C_{NAl} and C_{NAc} respectively.

3.6.4 Central compartment

The central compartment tissue water volume (TWV) is the sum of the TWVs of its components: blood, bone, brain, kidneys, lungs, skin, heart and spleen. The central compartment is modeled as a well-mixed venous pool with no chemical reaction. The mass balance equations for ethanol and acetaldehyde, respectively, for the central compartment are given by equations (A11) and (A12)

$$V_C\left(\frac{dC_{CAl}}{dt}\right) = -v_L(C_{CAl} - C_{LAl}) - v_M(C_{CAl} - C_{MAl}) \qquad \text{(A11)}$$

$$V_C\left(\frac{dC_{CAc}}{dt}\right) = -v_L(C_{CAc} - C_{LAc}) - v_M(C_{CAc} - C_{MAc}) \qquad \text{(A12)}$$

V_C is the total water volume for the central compartment, v_L is the liver blood flow rate, and v_M is the blood flow-rate to the muscle compartment.

3.6.5 Muscle and fat compartment

The muscle and fat compartment tissue water volume (TWV) is equal to the sum of TWVs of the muscle and fat tissues. The average perfusion rate for muscle and fat is 0.037 ml/min/mlH_2O, which is significantly smaller than the other tissues and therefore important to the kinetics of ethanol distribution and elimination. A mass balance on the muscle and fat compartment for ethanol and acetaldehyde gives equations (A13) and (A14), respectively.

$$V_M\left(\frac{dC_{MAl}}{dt}\right) = v_M(C_{CAl} - C_{MAl}) \qquad \text{(A13)}$$

$$V_M\left(\frac{dC_{MAc}}{dt}\right) = v_M(C_{CAc} - C_{MAc}) \qquad \text{(A14)}$$

V_M is the volume of the muscle and fat compartment, and v_M is the blood flow rate to the muscle and fat compartment.

3.7 Acknowledgments

We gratefully acknowledge Dr. Richard A. Deitrich (Department of Pharmacology, University of Colorado, Health Science Center) for helpful discussions.

3.8 References

Bass, L., Keiding, S., Winkler, K., & Tygstrup, N. (1976). Enzymatic elimination of substrates flowing through the intact liver. *J Theor Biol 61(2)*, 393-409.

Brien, J. F., & Loomis, C. W. (1983). Pharmacology of acetaldehyde. *Can J Physiol Pharmacol 61(1)*, 1-22.

Condouris, G. A., & Havelin, D. M. (1987). Acetaldehyde and cardiac arrhythmias. *Arch Int Pharmacodyn Ther 285(1)*, 50-9.

Deetz, J. S., Luehr, C. A., & Vallee, B. L. (1984). Human liver alcohol dehydrogenase isozymes: reduction of aldehydes and ketones. *Biochemistry 23(26)*, 6822-8.

Derr, R. F. (1993). Simulation studies on ethanol-metabolism in different human-populations with a physiological pharmacokinetic model. *Journal of Pharmaceutical Sciences 82(7)*, 677-682.

Enomoto, N., Takase, S., Yasuhara, M., & Takada, A. (1991). Acetaldehyde metabolism in different aldehyde dehydrogenase-2 genotypes. *Alcohol Clin Exp Res 15*, 141–144.

Fogler, H. S. (1999). *Elements of Chemical Reaction Engineering* (3rd ed.). Upper Saddle River, NJ: Prentice Hall.

Jones, A. W. (1995). Measuring and reporting the concentration of acetaldehyde in human breath. *Alcohol Alcohol 30(3)*, 271-85.

Jones, A. W., Neiman, J., & Hillbom, M. (1988). Concentration-time profiles of ethanol and acetaldehyde in human volunteers treated with the alcohol-sensitizing drug, calcium carbimide. *Br J Clin Pharmacol 25(2)*, 213-21.

Keiding, S., & Priisholm, K. (1984). Current models of hepatic pharmacokinetics: flow effects on kinetic constants of ethanol elimination in perfused rat liver. *Biochem Pharmacol 33(20)*, 3209-12.

Lands, W. E. M. (1998). A review of alcohol clearance in humans. *Alcohol 15(2)*, 147-160.

Larsen, O. A., Winkler, K., & Tygstrup, N. (1963). Extra plasma in liver calculated from hepatic hematocrit in patients with portacaval anastomosis. *Clinical Science 25(3)*, 357-360.

Levitt, D. G. (2002). PKQuest: measurement of intestinal absorption and first pass metabolism – application to human ethanol pharmacokinetics. *BMC Clin Pharmacol 2*, 4.

Levitt, M. D., & Levitt, D. G. (1994). The critical role of the rate of ethanol absorption in the interpretation of studies purporting to demonstrate gastric metabolism of ethanol. *J Pharmacol Exp Ther 269(1)*, 297-304.

Levitt, M. D., Li, R., DeMaster, E. G., Elson, M., Furne, J., & Levitt, D. G. (1997). Use of measurements of ethanol absorption from stomach and intestine to assess human ethanol metabolism. *Am J Physiol 273(4 Pt 1)*, G951-7.

Lucey, M. R., Hill, E. M., Young, J. P., Demo-Dananberg, L., & Beresford, T. P. (1999). The influences of age and gender on blood ethanol concentrations in healthy humans. *Journal of Studies on Alcohol 60(1)*, 103-110.

Lundquist, F., & Wolthers, H. (1958). The kinetics of alcohol elimination in man. *Acta Pharmacologica Et Toxicologica 14(3)*, 265-289.

Norberg (2001). Clinical pharmacokinetics of intraveneous ethanol: Relationship between the ethanol space and total body water. Stockholm, Sweden, Karolinska Institute.

Peng, G. S., Wang, M. F., Chen, C. Y., Luu, S. U., Chou, H. C., Li, T. K., & Yin, S. J. (1999). Involvement of acetaldehyde for full protection against alcoholism by homozygosity of the variant allele of mitochondrial aldehyde dehydrogenase gene in asians. *Pharmacogenetics 9(4)*, 463-476.

Riveros-Rosas, H., Julian-Sanchez, A., & Pina, E. (1997). Enzymology of ethanol and acetaldehyde metabolism in mammals. *Arch Med Res 28(4)*, 453-71.

Rowland, M., Tozer, T.N., & Rowland, R. (1995). *Clinical Pharmacokinetics, Concepts and Applications* (3rd. ed.). PA: Williams and Wilkins.

Shampine, L. F., & Reichelt, M. W. (1997). The MATLAB ODE suite. *SIAM J Sci Comput 18*, 1-22.

Wang, X. P., Sheikh, S., Saigal, D., Robinson, L., & Weiner, H. (1996). Heterotetramers of human liver mitochondrial (class 2) aldehyde dehydrogenase expressed in Escherichia coli - A model to study the heterotetramers expected to be found in oriental people. *Journal of Biological Chemistry 271(49)*, 31172-31178.

Widmark, E. (1932). *Die theoretischen Grundlagen und die praktische Verwendbarkeit der gerichtlich-medizinischen Alkoholbestimmung*. Berlin: Urban and Schwarzenberg.

Wilkinson, P. K., Sedman, A. J., Sakmar, E., Kay, D. R., & Wagner, J. G. (1977). Pharmacokinetics of ethanol after oral administration in the fasting state. *J Pharmacokinet Biopharm 5(3)*, 207-24.

Wynne, H. A. W., Wood, P., Herd, B., Wright, P., Rawlins, M. D., & James, O. F. W. (1992). The association of age with the activity of alcohol dehydrogenase in human liver. *Age and Aging 21*, 417-420.

Yamamoto, H., Tanegashima, A., Hosoe, H., & Fukunaga, T. (2000). Fatal acute alcohol intoxication in an *ALDH2* heterozygote: a case report. *Forensic Sci Int 112(2-3)*,201-7.

A.

ethanol	acetaldehyde
$CH_3CH_2OH + ADH \leftrightarrow CH_3CH_2OH \bullet ADH$ (NAD⁺/NADH)	$CH_3CHO + ALDH \leftrightarrow CH_3CHO \bullet ALDH$ (NAD⁺/NADH)
$CH_3CH_2OH \bullet ADH \leftrightarrow CH_3CHO \bullet ADH + H_2O$ (NAD⁺/NADH)	$H_2O + CH_3CHO \bullet ALDH \leftrightarrow CH_3COOH \bullet ALDH$ (NAD⁺/NADH)
$CH_3CHO \bullet ADH \leftrightarrow CH_3CHO + ADH$	$CH_3CHOOH \bullet ALDH \rightarrow CH_3COOH + ALDH$
$-r_{Al} = \frac{Vmax_{ADH}(C_{Al}) - Vrev_{ADH}(C_{Ac})}{Km_{ADH} + (C_{Al}) + Krev_{ADH}(C_{Ac})}$	$-r_{Ac} = \frac{Vmax_{ALDH}(C_{Ac})}{Km_{ALDH} + (C_{Ac})}$
$-r_{Al}$ = rate of dissapearance of ethanol	$-r_{Ac}$ = rate of dissapearance of acetaldehyde

B.

Stomach Compartment

$\left(\frac{dV_S}{dt}\right) = -k_S(V_S)$ k_S = stomach-emptying rate constant; V_S = volume of fluid in the stomach

ethanol	acetaldehyde
Gastrointestinal Compartment	
$V_G \frac{dC_{GAl}}{dt} = \left(\frac{2}{3}v_L\right)(C_{CAl} - C_{GAl}) + k_S(V_S)(C_{SAl})$	$V_G \frac{dC_{GAc}}{dt} = \left(\frac{2}{3}v_L\right)(C_{CAc} - C_{GAc})$
Liver Compartment	
$\Delta V_L \frac{dC_{NAl}}{dt} = v_L(C_{(N-1)Al} - C_{NAl}) + r_{Al}(C_{NAl}, C_{NAc})\Delta V_L$	$\Delta V_L \frac{dC_{NAc}}{dt} = v_L(C_{(N-1)Ac} - C_{NAc}) - r_{Al}(C_{NAl}, C_{NAc})\Delta V_L + r_{Ac}(C_{NAc})\Delta V_L$
Central Compartment	
$V_C\left(\frac{dC_{CAl}}{dt}\right) = -v_L(C_{CAl} - C_{LAl}) - v_M(C_{CAl} - C_{MAl})$	$V_C\left(\frac{dC_{CAc}}{dt}\right) = -v_L(C_{CAc} - C_{LAc}) - v_M(C_{CAc} - C_{MAc})$
Muscle Compartment	
$V_M\left(\frac{dC_{MAl}}{dt}\right) = v_M(C_{CAl} - C_{MAl})$	$V_M\left(\frac{dC_{MAc}}{dt}\right) = v_M(C_{CAc} - C_{MAc})$

v_L = liver flow rate
V_i = tissue water volume in i-th compartment
C_{iAl} = ethanol concentration in i-th compartment
C_{iAc} = acetaldehyde concentration in i-th compartment

Fig. 3.1. A. Derivation of rate laws for ethanol and acetaldehyde. Adapted from (1) F. Lundquist & H. Wolthers, The kinetics of alcohol elimination in man, *Acta Pharmacologica Et Toxicologica 14(3)*, pp. 265–289, copyright 1958, with permission of Munksgaard International Publishers and (2) H. Riveros-Rosas, A. Julian-Sanchez, & E. Pina, Enzymology of ethanol and acetaldehyde metabolism in mammals, *Archives of Medical Research 28(4)*, pp. 453–471, copyright 1997, with permission of Elsevier. B. Mass balance equations for physiologically based model.

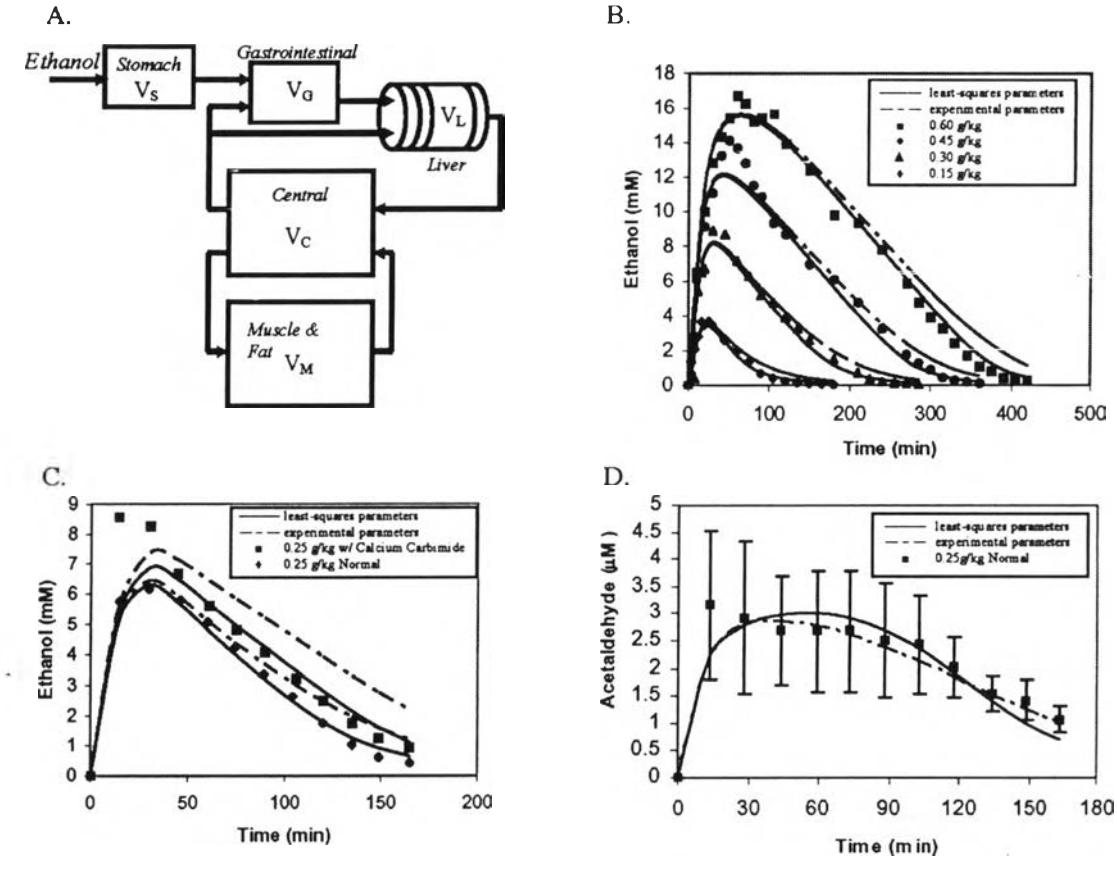

Fig. 3.2. A. Compartment and perfusion diagram for model. Perfusion interactions between compartments are shown by black arrows. V_G, V_L, V_C, and V_M are tissue water volumes for the gastrointestinal tract, liver, central, and muscle compartments, respectively. V_S is the stomach contents volume. B. Observed data (Wilkinson et al., 1977) versus model–predicted blood ethanol curves after ingestion of four different doses of ethanol in adult white male subjects. C. Observed data (Jones et al., 1988) versus model–predicted blood ethanol curves after ingestion of a 0.25-g/kg dose of 96% ethanol in 10 adult male subjects. D. Observed data (Jones et al., 1988) versus model–predicted blood acetaldehyde curve after ingestion of a 0.25-g/kg dose of ethanol in 10 adult male subjects. Error bars shown are one standard deviation of the mean of Jones et al. (1988) data. Note: All doses in panels B–D were adjusted from the 74.5-kg subjects to the "standard" 69.4-kg man used in the model. Observed data, panel B: adapted from P. K. Wilkinson, A. J. Sedman, E. Sakmar, D. R. Kay, & J. G. Wagner, Pharmacokinetics of ethanol after oral administration in the fasting state, *Journal of Pharmacokinetics and Biopharmaceutics 5(3)*, pp. 207–224, fig. 6,

copyright 1977, with permission of Kluwer. Observed data, panels C and D: adapted from A. W. Jones, J. Neiman, & M. Hillbom, Concentration–time profiles of ethanol and acetaldehyde in human volunteers treated with the alcohol-sensitizing drug, calcium carbimide, *British Journal of Clinical Pharmacology 25(2)*, pp. 213–221, fig.2 & fig. 3, copyright 1988, with permission of Blackwell Publishing.

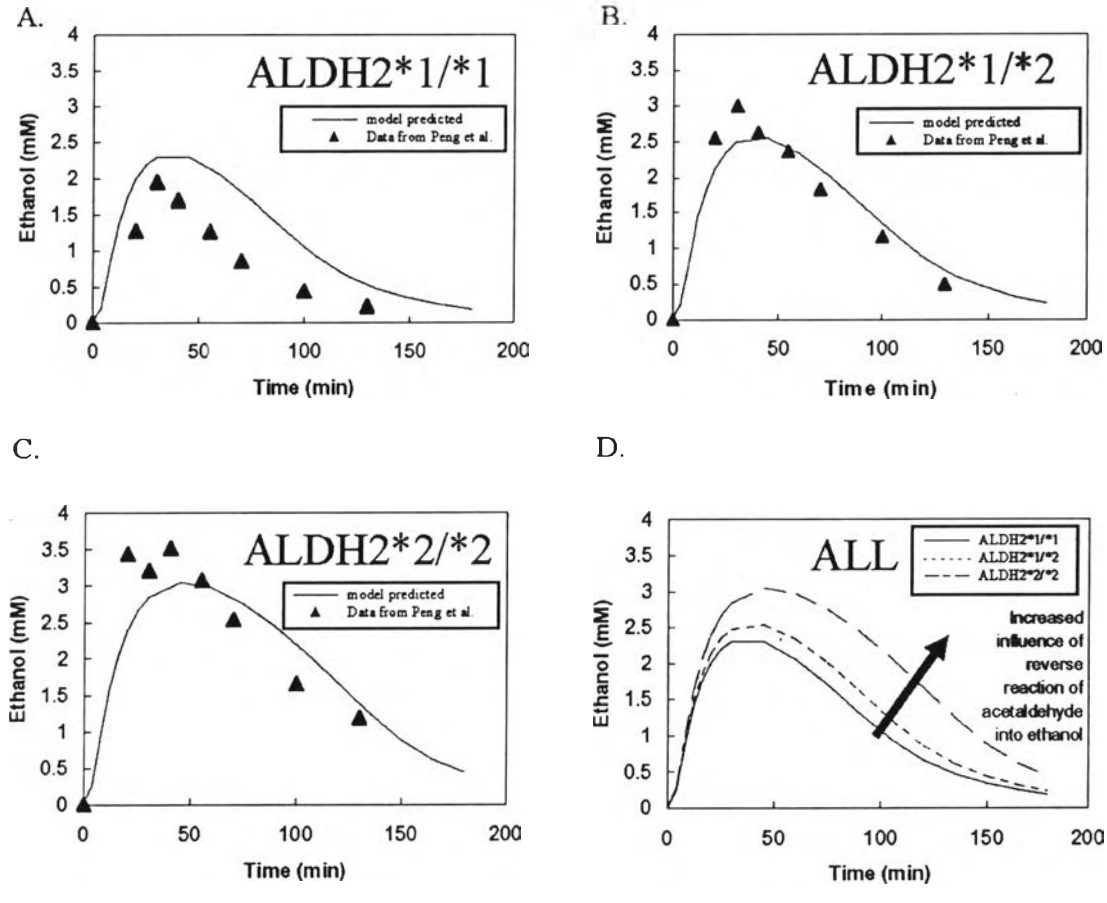

Fig. 3.3. Ethanol concentration results for model (——) versus data (▲) from Peng et al. (1999) after an equivalent 0.2-g/kg dose of ethanol in normal (A) normal *ALDH2*1/*1*, (B) heterozygous *ALDH2*1/*2*, and (C) homozygous *ALDH2*2/*2* individuals. D. Comparison of the model-predicted ethanol concentration results from cases *ALDH2*1/*1* (————), *ALDH2*1/*2* (- - - - -), and *ALDH2*2/*2* (— — —) to illustrate the effect of the reverse reaction of acetaldehyde to ethanol. Data (▲), panels A–C: adapted from G. S. Peng, M. F. Wang, C. Y. Chen, S. U. Luu, H. C. Chou, T. K. Li, & S. J. Yin, Involvement of acetaldehyde for full protection

against alcoholism by homozygosity of the variant allele of mitochondrial aldehyde dehydrogenase gene in Asians, *Pharmacogenetics 9(4)*, pp. 463–476, fig. 1, copyright 1999, with permission of Lippincott Williams & Wilkins.

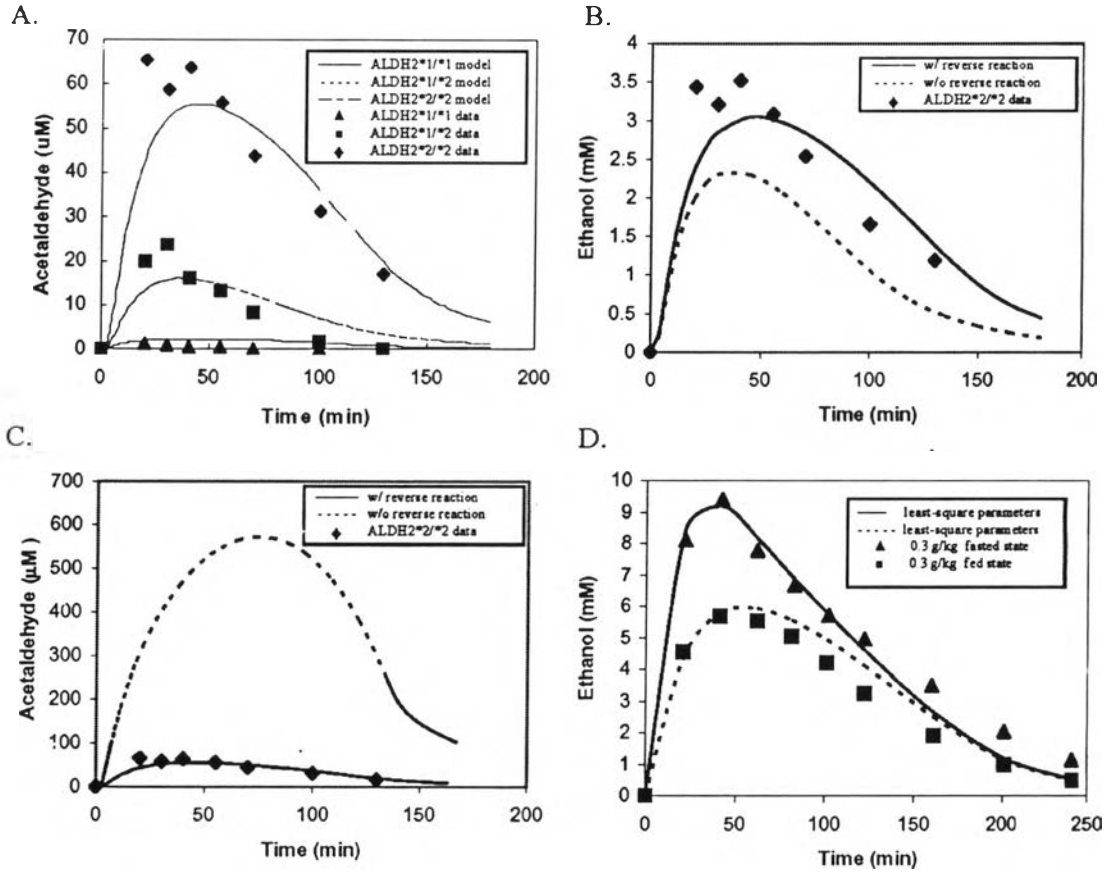

Fig. 3.4. A. Acetaldehyde concentration data from Peng et al. (1999) after an equivalent 0.2 g/kg dose of ethanol in normal *ALDH2*1/*1* data (▲); model (————), heterozygous *ALDH2*1/*2* data (■); model (- - - - - -), and homozygous *ALDH2*2/*2* data (♦); and model (— — —). B. Ethanol concentration data from Peng et al. (1999) after an equivalent 0.2-g/kg dose of ethanol/kg with homozygous *ALDH2*2/*2* data (♦) shown. Model curves are shown for homozygous *ALDH2*2/*2* with reverse reaction (——) and without reverse reaction (- - - - - -). C. Acetaldehyde concentration data from Peng et al. (1999) after an equivalent 0.2-g/kg dose of ethanol in subjects homozygous *ALDH2*2/*2* (♦). Model curves are shown for homozygous *ALDH2*2/*2* with reverse reaction (——) and without reverse reaction (- - - - - -). Note the completely different behavior and peak value of

acetaldehyde for the case without the reverse reaction. D. Ethanol concentration data from Lucey et al. (1999) after an overnight fast (▲) and after a standard meal (■). Also shown are model-predicted blood ethanol curves after an overnight fast (——) and after a standard meal (- - - - - -). Doses were adjusted from the 77.2-kg subjects to the "standard" 69.4 kg-man used in the model. Data from Peng et al. (1999), panels A–C: adapted from G. S. Peng, M. F. Wang, C. Y. Chen, S. U. Luu, H. C. Chou, T. K. Li, & S. J. Yin, Involvement of acetaldehyde for full protection against alcoholism by homozygosity of the variant allele of mitochondrial aldehyde dehydrogenase gene in Asians, *Pharmacogenetics 9(4)*, pp. 463–476, fig. 1, copyright 1999, with permission of Lippincott Williams & Wilkins. Data from Lucey et al. (1999): adapted from M. R. Lucey, E. M. Hill, J. P. Young, L. Demo-Dananberg, & T. P. Beresford, The influences of age and gender on blood ethanol concentrations in healthy humans, *Journal of Studies on Alcohol 60(1)*, pp. 103–110, fig. 1c, copyright 1999, with permission of Center on Studies of Alcohol, Rutgers University.

Table 3.1

Tissue water volumes, flow rates, and perfusion rates for the "standard" 69.4-kg man

Compartment	Tissue	H_2O volume (l)	Blood flow (ml/min)	Perfusion rate (ml/min/ml H_2O)	Residence time (min)	Source
Central V_C = 11.56 l	Lungs	0.37	5,000	13.33	0.07	A
	Kidneys	0.21	1,100	5.14	0.19	A
	Blood	2.84	5,000	1.76	0:57	A
	Brain	1.03	700	0.68	1.47	A
	Heart, spleen	1.18	350	0.29	3.37	A
	Bone	2.44	250	0.10	10.00	A
	Skin	3.49	300	0.085	11.63	A
Muscle	Fat	3.76	200	0.053	18.80	A
V_M = 25.76 l	Muscle	22.0	750	0.034	29.33	A
Gastrointestinal tract V_G = 2.4 l	Stomach/ intestine	2.40	900	0.375	2.67	a,b
Liver V_L = 1.08 l	Liver	1.08	1,350	1.25	0.80	a,c

Total body water content is 40.8 l.

[a]Adapted from M. Rowland, T. N. Tozer, & R. Rowland, *Clinical Pharmacokinetics: Concepts and Applications*, tbl. 6, copyright 1995, with permission of Lippincott Williams & Wilkins.

[b]Adapted from R. F. Derr, Simulation studies on ethanol metabolism in different human populations with a physiological pharmacokinetic model, *Journal of Pharmaceutical Sciences 82(7)*, pp. 677–682, copyright 1993, with permission of John Wiley & Sons.

[c]Adapted from O. A. Larsen, K. Winkler, & N. Tygstrup, "Extra" plasma in the liver calculated from hepatic hematocrit in patients with portacaval anastomosis, *Clinical Science 25(3)*, pp. 357–360, tbl. 4, copyright 1963, with permission of Portland Press Ltd.

Table 3.2

Rate-law parameters with the best model fit from least-squares analysis compared with experimentally observed ranges and values used for the comparison plots

Parameter	Model	Experimental	Graph	Units	Source
V_{maxAl}	2.2	2.0, 2.4–4.7[†]	2.2	mmol*(min*kg liver)$^{-1}$	a,b
K_{mAl}	0.4	~1	1	mM	c
V_{rev}	32.6	11–110[‡]	60.5	mmol*(min*kg liver)$^{-1}$	d
K_{rev}	1	~1	1	mM/mM	d,e
V_{maxAc}	2.7	-	2.7	mmol*(min*kg liver)$^{-1}$	Estimate
K_{mAc}	1.2	0.2–3	1.6	μM	c,f

[†]Experimental values of 2.4 and 4.7 mmol*(min*kg liver)$^{-1}$ were observed at pH 8.5 and 10.5, respectively. Actual activity at physiologic liver pH of 7.5 is expected to be lower because pH 8.5 and 10.5 correspond to the optimal pH of two different forms of alcohol dehydrogenase.

‡Calculated on basis of a 5- to 50-fold increase in kcat values of forward reaction V_{maxAl}.

[a]Adapted from R. F. Derr, Simulation studies on ethanol metabolism in different human populations with a physiological pharmacokinetic model, *Journal of Pharmaceutical Sciences 82(7)*, pp. 677–682, copyright 1993, with permission of John Wiley & Sons.

[b]Adapted from H. A. W. Wynne, P. Wood, B. Herd, P. Wright, M. D. Rawlins, & O. F. W. James, The association of age with the activity of alcohol dehydrogenase in human liver, *Age and Ageing 21(6)*, pp. 417-420, tbl. Hepatic ADH activity, copyright 1992, with permission of Oxford University Press.

[c]Adapted from H. Riveros-Rosas, A. Julian-Sanchez, & E. Pina, Enzymology of ethanol and acetaldehyde metabolism in mammals, *Archives of Medical Research 28(4)*, pp. 453–471, tbl. 4 & 6, copyright 1997, with permission of Elsevier.

[d]Adapted from W. E. M. Lands, A review of alcohol clearance in humans, *Alcohol 15(2)*, pp. 147–160, tbl. 1, copyright 1998, with permission of Elsevier.

[e]Adapted from J. S. Deetz, C. A. Luehr, & B. L. Vallee, Human liver alcohol dehydrogenase isozymes: reduction of aldehydes and ketones, *Biochemistry 23(26)*, pp. 6822–6828, tbl. II, copyright 1984, with permission of the American Chemical Society.

[f]Adapted from G. S. Peng, M. F. Wang, C. Y. Chen, S. U. Luu, H. C. Chou, T. K. Li, & S. J. Yin, Involvement of acetaldehyde for full protection against alcoholism by homozygosity of the variant allele of mitochondrial aldehyde dehydrogenase gene in Asians, *Pharmacogenetics 9(4)*, pp. 463–476, copyright 1999, with permission of Lippincott Williams & Wilkins.

Table 3.3

Stomach-emptying rate constants.

	Ethanol			
Study/source	0.15 g/kg	0.3 g/kg	0.45 g/kg	0.6 g/kg
Current work, k_s	0.047	0.040	0.032	0.025
Wilkinson et al.[a], k_s	0.055	0.018	0.009	0.005

[a]Adapted from P. K. Wilkinson, A. J. Sedman, E. Sakmar, D. R. Kay, & J. G. Wagner, Pharmacokinetics of ethanol after oral administration in the fasting state, *Journal of Pharmacokinetics and Biopharmaceutics 5(3)*, pp. 207–224, copyright 1977, with permission of Kluwer.